

RESEARCH ARTICLE | JANUARY 06 2012

## Immobilization of mycotoxins on modified nanodiamond substrates

N. M. Gibson; T. J. M. Luo; D. W. Brenner; O. Shenderova

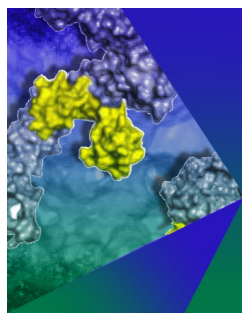


*Biointerphases* 6, 210–217 (2011)

<https://doi.org/10.1116/1.3672489>



CrossMark



### Biophysics Reviews

**Call for Applicants**

Seeking New Associate Editor



# Immobilization of mycotoxins on modified nanodiamond substrates

N. M. Gibson, T. J. M. Luo,<sup>a)</sup> and D. W. Brenner

Department of Materials Science and Engineering, North Carolina State University, 911 Partners Way, Raleigh, North Carolina 27695

O. Shenderova

International Technology Center, P.O. Box 13740, Research Triangle Park, North Carolina 27709

(Received 23 September 2011; accepted 7 December 2011; published 6 January 2012)

The effectiveness of modified nanodiamonds (NDs) for the adsorption of mycotoxins, aflatoxin B1 (AfB1) and ochratoxin A (OTA), are investigated in this paper. Binding and release mechanisms of the mycotoxins were addressed using an assortment of NDs modified by different surface treatments, including carboxylation, hydrogenation and hydroxylation, followed by isolating NDs of different sizes. Results indicate that AfB1 adsorption on NDs is directly related to aggregate size, whereas OTA adsorption is primarily centered upon electrostatic interactions that depend on the types of surface functional groups on the ND. Findings show that modified NDs with small aggregation sizes (~40 nm) have greater adsorption capacities for AfB1 than yeast cells walls and untreated NDs from various vendors, but comparable to activated charcoal. In OTA studies, positively charged NDs outperformed clay minerals, which are well-known and efficient sorbents for mycotoxins. Furthermore, ND adsorption capacities can be preserved in a wide range of pH. © 2011 American Vacuum Society. [DOI: 10.1116/1.3672489]

## I. INTRODUCTION

Each year approximately 25% of the world's cereals are contaminated by mycotoxins, secondary metabolites produced by fungi, and enter the food chain through direct ingestion or consumption of tainted animal products, i.e., meat and milk.<sup>1-5</sup> Ingestion of mycotoxins has been linked to toxicosis, cancer,<sup>6,7</sup> and even, death.<sup>8</sup> Two well-known and detrimental mycotoxins are aflatoxin B1 (AfB1) and ochratoxin A (OTA) [Fig. 1(a) and 1(b)]. AfB1 has been identified as one of the most carcinogenic naturally occurring compounds<sup>9</sup> and commonly infects cereals, tree nuts, oilseeds and spices that grow in warm, humid settings.<sup>10,11</sup> AfB1 is classified as a group 1 carcinogen due to gastrointestinal (GI) enzymes which breakdown AfB1 into epoxylated derivatives that form adducts with DNA,<sup>12-14</sup> thereby causing heritable changes that lead to malignant cell formation particularly in hepatic cells.<sup>15</sup> OTA, while less potent than AfB1, receives much attention due to the ability of the producing fungi to proliferate in low temperatures (0 to 31 °C) and humidities, and in a wide range of pH (pH 2 to 10).<sup>16</sup> Consequently, OTA is found in crops worldwide, though it is most common in Northern Africa, North America and Europe.<sup>17,18</sup> In fact, evidence of OTA in Europeans' blood and breast milk was found to be widespread,<sup>19,20</sup> with exposure primarily gained through ingestion of grains (58% of the intake), wine (21%), grape juice (7%), coffee (5%) and pork (3%).<sup>21</sup> Unlike AfB1, OTA accumulates in tissue and has been associated with mutagenic, nephrotoxic, nephrocarcinogenic, teratogenic<sup>22</sup> and immunosuppressive

properties that may lead to the development of certain diseases, such as balkan endemic nephropathy (BEN), urinary tract tumors and possibly testicular cancer.<sup>23</sup>

While these mycotoxins have long been identified, there has been no economical, easy and practical resolution for removing these toxins from contaminated crops and feedstuff. Methods to remove or decompose mycotoxins in crops have included physical, chemical, and biological means; however, the procedures vary in their effectiveness<sup>24,25</sup> and may discolor and/or decay nutritional contents of the foodstuff.<sup>26-28</sup> The most recent treatment is the use of non-nutritive binding agents, termed enterosorbents, which adsorb and remove the mycotoxins within the GI tract before absorption into the body. Several enterosorbents have been considered for mycotoxins adsorption, including activated charcoal, yeast cells and clay minerals, but due to their inability to bind a wide variety of toxins<sup>2,4</sup> or concerns in vitamin and mineral uptake,<sup>2,3</sup> alternative enterosorbent materials are being explored.

Nanodiamond particles (NDs), produced through detonation synthesis, are a prospective enterosorbent material<sup>29,30</sup> due to their high dispersivity, which allows for easy administration and quantifiable dosing through water substitutions. In addition, their colloidal stability and sorption capacities are preserved over a wide pH range, important for interacting in the GI tract.<sup>29,30</sup> Furthermore, NDs have been shown to be biocompatible and nontoxic in a variety of *in vitro* and *in vivo* studies.<sup>31-33</sup> Lastly, because NDs can be tailored with different functional groups during manufacturing and modification treatments, NDs may be able to selectively adsorb AfB1 and OTA while excluding critical nutrients. This paper reports results from assessing AfB1 and OTA adsorption on NDs modified under variety of treatments,

<sup>a)</sup> Author to whom correspondence may be addressed; electronic mail: tluo@ncsu.edu

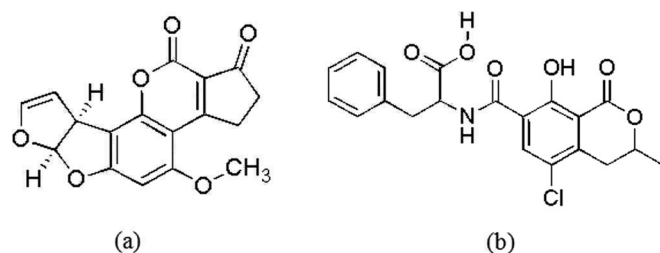


FIG. 1. Chemical Structure of (a) aflatoxin B1 (AfB1) and (b) ochratoxin A (OTA).

including surface termination by hydrogen, carboxyls and hydroxyl groups, as well as determining possible mechanisms of interaction.

## II. EXPERIMENTAL PROCEDURES

### A. Nanodiamonds

Nanodiamond particles used in this work were synthesized at the manufacturers site by the detonation of a mixture of trinitrotoluene (TNT) and 1,3,5-trinitro-1,3,5-*s*-triazine (RDX), followed by treatment in liquid or gas-phase oxidizers to reduce nondiamond carbon content. The list of NDs used in our experiments is summarized in Table I. Complete details of manufacturing and hydrosol preparations for Ch-st, I6, RUDDM1, RDDM and ozonated NDs (OZ-ND) have previously been reported.<sup>29,30,34,35</sup> Here, only brief processing methods will be discussed. Ch-st ND (New Technologies, Chelyabinsk, Russia) was purified using a solution of chromic anhydride in sulfuric acid. I6-140 samples were produced from Ch-st through treatment in H<sub>2</sub>O<sub>2</sub>/NaOH, ion-exchange, then fractionating. RUDDM1 (Real-Dzerzinsk, LTD, Russia), was obtained by purifying detonation soot by singlet atomic oxygen in the base environment, followed by treatment in nitric acid, NaCl and fractionation. I6-220 and I6-40 samples were obtained by centrifugal separation of I6-140 sample, with the number corresponding to the aggregate size. RUDDM1, which has been used previously for

adsorption experiments, was also fractionated to a 40 nm particle size. RDDM (Real-Dzerzinsk) was produced by detonation of graphite precursors mixed with RDX and fractionated by centrifugation. Ozonated ND (OZ-ND, New Technologies) was obtained by treating detonation soot with ozone at 200 °C. OZ-B1, obtained through centrifugation, represents the smaller fractions of the OZ-ND sample. Porous NDs, selected to determine the influence of pores on toxin adsorption, were produced by Alit, Ukraine, by high temperature high pressure compacting of detonation NDs.<sup>36</sup> Finally, surface functionalization was conducted on the I6-140 sample to form hydrogenated (I6-H), hydroxylated (I6-OH) and carboxylated (I6-COOH) derivatives. In the current approach, hydroxylation was achieved using reduction with lithium aluminum hydride.<sup>37</sup> ND-COOH was produced by air treatment at 430 °C for 1 hr, followed with treatment in HCl for 1 hr and washing. ND-H was created through treatment in H<sub>2</sub> flow for three days at 450 °C.

Surface groups of NDs used in the paper were previously confirmed using FTIR and XPS techniques.<sup>29,31,37</sup> Supplementary surface characterization techniques, via thermal desorption mass spectrometry (TDMS) and time-of-flight secondary ion mass spectrometry (TOF-SIMS), have also supported these results and have helped to differentiate between particular surface groups, i.e., carboxyls versus anhydrides.<sup>38</sup> Due to ND's varying surfaces, which stem from different manufacturing procedures, ND's acquire different zeta potentials (ZPs) and vary in their aggregate sizes. Before measuring ZP and aggregate size, NDs were suspended in deionized (DI) water at a 0.1 wt. % concentration using rigorous ultrasonication.<sup>29</sup> Particle size distributions were determined by dynamic light scattering (DLS) on the Malvern ZetaSizer NanoZS, and confirmed using the Beckman Coulter N5 submicron particle size analyzer. Samples were diluted for measurement by adding 10 μL of the prepared 0.1 wt. % suspension to approximately 1 mL of DI water. Unimodal intensity-based sizes (Z-average sizes) are reported. ZP measurements, conducted also on the Zetasizer,

TABLE I. NDs used in adsorption experiments with related particle diameter measurements (nm), zeta potentials (ZP, mV) and a brief description of processing methods.

ND Type	Size, nm	ZP, mV	Processing
Ch-st	298.8	19.0	CrO <sub>3</sub> in H <sub>2</sub> SO <sub>4</sub>
I6-220	219.1	44.6	Ch-st; NaOH+H <sub>2</sub> O <sub>2</sub> ; ion-exchange resin; FC*
I6-140	140.2	47.7	Ch-st; NaOH+H <sub>2</sub> O <sub>2</sub> ; ion-exchange resin; FC
I6-40	40.0	50.1	Ch-st; NaOH+H <sub>2</sub> O <sub>2</sub> ; ion-exchange resin; FC
I6-H	128.3	68.1	I6-140; H <sub>2</sub>
I6-OH	128.1	52.6	I6-140; air treatment; HCl
I6-COOH	145.5	-59.4	I6-140; reduction with lithium aluminum hydride
Porous	177.4	-38.1	High temperature-high pressure compacting of NDs
RDDM	175.9	-46.1	Graphite precursors; FC
OZ-ND	175.0	-44.6	Soot oxidized with Ozone
OZ-B1	80.8	-51.2	Soot oxidized with Ozone; FC
RUDDM1	79.8	-49.2	Singlet O in NaOH; HNO <sub>3</sub> ; NaCl; FC
RUDDM1-40	40.1	-53.3	Singlet O in NaOH; HNO <sub>3</sub> ; NaCl; FC

\*FC: Fractionation by Centrifugation.

were conducted by injecting 1.5 mL of the undiluted ND suspension into Malvern supplied capillary cells. Using Laser Doppler Microelectrophoresis, electrophoretic mobility was measured. ZP was derived from the measured electrophoretic mobility using the Smoluchowski's approximation for Henry's function, the latter equals 1.5, which is justified by the relatively large size of the particles. The reported results for both the size and ZPs are averaged over three measurements performed at 25 °C. For select NDs specific surface areas (SSAs) were also performed using Brunauer, Emmett and Teller (BET) method, which used nitrogen adsorption at 77 K (Quadrasorb from Quantachrome).

## B. Aflatoxin B1 Studies

AfB1 [purchased from Sigma Aldrich, Fig. 1(a)] stock solution was prepared for adsorption studies by dissolving pure AfB1 crystals in acetonitrile, followed by dilution in DI water to yield a final concentration of 10 µg/mL. Using the batch isotherm procedure, where a fixed amount of adsorbent is exposed to increasing concentrations of the solute, 0.3 mL of ND suspension (0.1 wt. %, prepared using the aforementioned method) was placed in a microcentrifuge tube. To this, 0.7 mL of AfB1 solution of varying concentrations (0.5 to 10 µg/mL) was added to make the total volume 1 mL. This mixture is noted as a 3:7 (ND:AfB1 v/v) ratio in later discussions. The ND-AfB1 mixture was then incubated at room temperature on an orbital shaker. Although adsorption reaches equilibrium within 5 mins, as confirmed by earlier studies,<sup>30,35</sup> 15 min incubation times were selected with current experiments. Longer incubation times did not lead to increased adsorption. Before centrifugation (14 000 rpm, 25 min, 25 °C) 0.162 µL of 0.3 g/mL NaCl solution was added to the ND-AfB1 suspension to help sediment the NDs, an imperative step for 40 nm NDs due to their exceptional colloidal stability. It was previously established that the introduction of the NaCl solutions does not interfere with adsorption of AfB1,<sup>35</sup> this is also true for the salt concentrations used in this paper. Following centrifugation, the supernatants were collected and the final equilibrium concentrations of unbound AfB1 were detected with UV-Vis spectroscopy. The amount of adsorbed AfB1 was estimated by the difference between the initial quantity of AfB1 and the unbound molecules in the supernatant (Fig. 2). Sample pellets made up of NDs with adsorbed molecules were saved for desorption studies. All samples were prepared and measured three times. Two control samples were prepared and tested in the same manner. Control samples included 0.3 mL of ND with 0.7 mL DI water (Control 1) and 0.3 mL DI water with 0.7 mL stock AfB1 (Control 2). The supernatant of Control 1 allowed for subtraction of any residual NDs in the UV-Vis spectra of the ND-AfB1 supernatant. Whereas, Control 2 was used as the reference point for determining the quantity of AfB1 adsorbed.

Several NDs were selected for construction of their corresponding adsorption isotherms (Fig. 3) by fitting UV-Vis adsorption data to the Langmuir equation (Table II). The

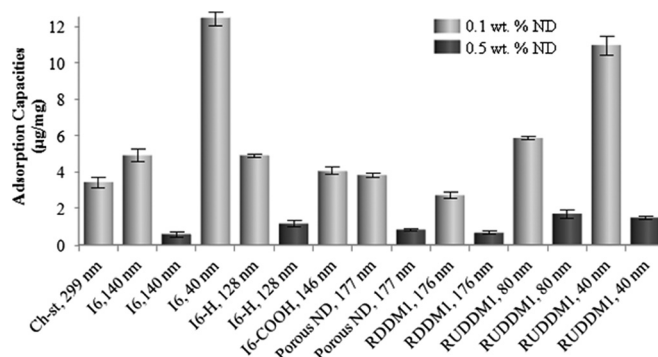


Fig. 2. Results of AfB1 adsorption on various ND substrates showing different adsorption capacities based on treatments and aggregate sizes (nm).

isotherm was plotted as adsorption capacity, or the quantity of adsorbed AfB1 (µg/mg), versus the equilibrium concentration of AfB1 (µg/mL). The Langmuir equation was also fitted to data using linear regression transforms, i.e., Eadie-Hofstee, Lineweaver-Burk, Reciprocal Line, and Scatchard (Table II). The slopes and intercepts from these plots gave rise to additional information such as the maximum capacity ( $Q_{max}$ ), indicating the greatest amount of AfB1 able to be adsorbed by 1 mg of ND, and the equilibrium constant ( $K$ ), which provided a description of the binding strength of the adsorption molecules to the ND substrate. Curves in the isotherm show best fits of the Langmuir equation to experimental data by using nonlinear least squares (NLLS) regression, whereas Table III shows comparisons of  $Q_{max}$  and  $K$  estimates of AfB1 on several different NDs. Additional research was completed by observing the effects on adsorption capacities when ND concentrations were increased from 0.1 wt. % to 0.5 wt. %, and by altering ND:AfB1 volume ratios from 3:7 to 1:1 and 3:1 (Fig. 4). Suspension concentrations used for the comparison of ND-AfB1 ratios were 5 mg/mL for NDs and 10 µg/mL for AfB1; all other preparation methods remained unchanged. To observe the influences of pH on adsorption, ND suspensions were adjusted to pH 2 and pH 11.5 using HCl or NaOH, prior to AfB1 additions. The control sample was prepared by mixing 0.7 mL of the AfB1 suspension and 0.3 mL of DI water at the appropriate pH. Because UV-Vis spectra indicated a degradation of the AfB1 molecule in the presence of NaOH, a separate experiment looking at the kinetics of AfB1 degradation was

TABLE II. Isotherm Equations used in curve fitting of AfB1 and OTA adsorption on NDs.

Langmuir Model (LM)	$q = Q_{max}(KC_w/1 + KC_w)$
Eadie-Hofstee (EHT)	$q = Q_{max} - (1/K)(q/C_w)$
Lineweaver-Burk Transform (LBT)	$1/q = 1/Q_{max} + (1/(KQ_{max}))(1/C_w)$
Reciprocal Langmuir Transform (RLT)	$C_w/q = (1/(KQ_{max})) + (1/Q_{max})C_w$
Scatchard Transform (ST)	$q/C_w = KQ_{max} - Kq$

$q$  = concentration of mycotoxin adsorbed (µg/mg)

$C_w$  = equilibrium concentration of mycotoxin.

$Q_{max}$  = maximum capacity (µg/mg)

$K$  = equilibrium constant

TABLE III. Maximum capacity ( $Q_{\max}$ ,  $\mu\text{g}/\text{mg}$ ) and equilibrium constants ( $K$ ,  $\text{mg}/\mu\text{g}$ ) of AFB1 on various NDs based on four Langmuir transform equations.

Transforms	RUDDM1-40		RUDDM1-40		I6-40		I6-COOH	
	0.5 wt. %		0.1 wt. %		0.1 wt. %		0.1 wt. %	
	$Q_{\max}$ ( $\mu\text{g}/\text{mg}$ )	$K$ ( $\text{mg}/\mu\text{g}$ )	$Q_{\max}$ ( $\mu\text{g}/\text{mg}$ )	$K$ ( $\text{mg}/\mu\text{g}$ )	$Q_{\max}$ ( $\mu\text{g}/\text{mg}$ )	$K$ ( $\text{mg}/\mu\text{g}$ )	$Q_{\max}$ ( $\mu\text{g}/\text{mg}$ )	$K$ ( $\text{mg}/\mu\text{g}$ )
Eadie-Hofstee	2.435	0.1470	9.306	0.4042	12.774	0.3183	6.522	0.2842
Lineweaver-Burk	2.895	0.1203	10.341	0.3729	12.485	0.3106	6.468	0.2883
Reciprocal Line	2.807	0.1243	9.234	0.4227	12.853	0.3265	6.596	0.2779
Scratchard	2.851	0.1222	10.119	0.3846	11.767	0.3724	6.606	0.2999
<b>Average</b>	<b>2.747</b>	<b>0.1290</b>	<b>9.750</b>	<b>0.3961</b>	<b>12.470</b>	<b>0.3320</b>	<b>6.548</b>	<b>0.2880</b>

performed. Directly after adjusting 5 mL of AFB1 solution to pH 11 the UV-Vis spectrum of the solution was repeatedly measured. Data were observed and recorded from ten seconds to 21 hs after pH adjustment (See supplementary material figure, SMFig. 1, Ref. 39). Final experiments observed toxin desorption by redispersing AFB1 bound ND pellets in 1 mL of DI water with 15 seconds of sonication, before centrifugation and UV-Vis detection. Redispersion procedures were repeated two more times for each sample in 1 mL of 5 mg/mL NaCl solution or 5 mg/mL  $\text{CaCl}_2$  solution to observe the role of ionic influences.

### C. Ochratoxin A Studies

OTA [Sigma Aldrich, Fig. 1(b)] was dissolved in methanol followed by dilution in DI water to obtain a final concentration of 10  $\mu\text{g}/\text{mL}$ . To 0.3 mL of ND suspension (0.1 wt. %) 0.7 mL of OTA was added to give a 3:7 (ND:OTA v/v) ratio. The mixture was incubated for 15 mins followed by centrifugation. In OTA studies, NaCl additions to sediment NDs were excluded, as salt in the presence of OTA (in the absence of ND) resulted in a secondary peak at 383 nm and a slight reduction in the 363 nm primary peak (See supplementary material, SMFig. 2, Ref. 39) This phenomena is discussed further in the results section. By

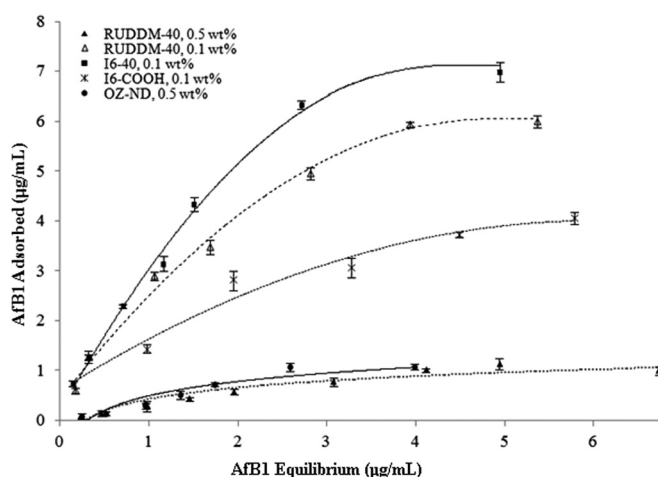


Fig. 3. Langmuir isotherm for AFB1 on various ND substrates and at different ND concentrations.

excluding salt, only larger ND aggregates could be used, since smaller aggregates will not allow for pellet formation during centrifugation.

Adsorption data comparing different NDs (Fig. 5) was performed by using the undiluted OTA stock solution. Langmuir isotherms were created using the same principles as in AFB1 studies, but varying the concentration of OTA from 2 to 10  $\mu\text{g}/\text{mL}$  (Fig. 6). Maximum capacities and equilibrium constants were found using the linear regression transforms listed in Table II and their results are reported in Table IV. pH experiments were also conducted to observe the resulting influence on OTA adsorption. Similar to AFB1 studies, ND suspensions were prepared to pH 2 and pH 10 before introducing OTA. All other steps remained unchanged. OTA desorption experiments were conducted using water and NaCl or  $\text{CaCl}_2$  solutions (3 redispersion cycles for each sample) in a manner identical to AFB1 studies.

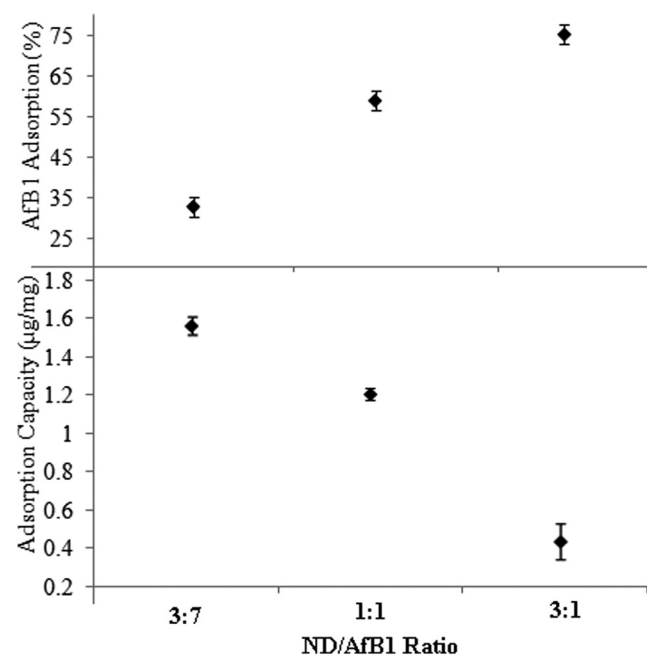


Fig. 4. Effect of ND:AfB1 volume ratios on adsorption percentage and capacity. Suspension concentrations were 5 mg/mL for NDs and 10  $\mu\text{g}/\text{mL}$  for AFB1.

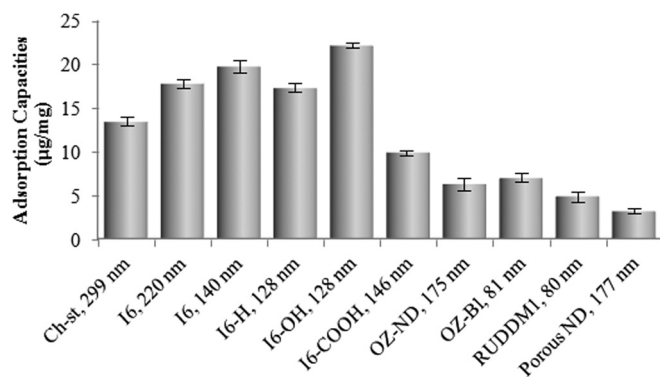


Fig. 5. Results of OTA adsorption on various ND substrates (0.1 wt. %) showing different adsorption capacities based on treatments and aggregate sizes (nm).

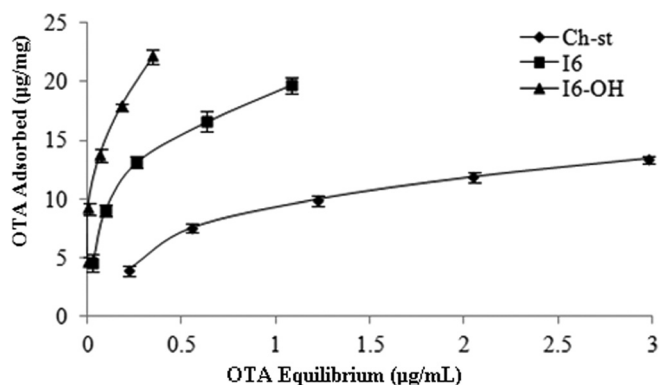


Fig. 6. Langmuir isotherm for OTA on Ch-st, I6-140 and I6-OH substrates (0.1 wt. %).

### III. RESULTS AND DISCUSSION

#### A. Aflatoxin B1

The initial evaluations of AFB1 adsorption by various ND substrates (Fig. 2) indicate that adsorption is dominated by aggregate size. Smallest ND aggregates (I6-40 and RUDDM1-40) exhibited the highest adsorption capacities due to their increased specific surface areas (SSAs), a result of size reduction. The polarity of the NDs seem to be an insignificant factor for the adsorption of AFB1, as both positively and negatively charged NDs bind approximately same amount of molecule, i.e., I6-40 nm and RUDDM1-40 nm (Fig. 2). Although AFB1 is considered to be a charge-neutral molecule, it contains both partial positive and negative species within its structure. Its dicarbonyl [Fig. 1(a)] can carry a partial positive charge, which has been shown to be attracted to negative sites on hydrated sodium aluminosilicate (HSCAS) enterosorbents.<sup>40,41</sup> With NDs however, it was observed that when comparing two equally sized aggregates the one with the positive ZP binds slightly higher amounts of AFB1 (Fig. 2). Consequently, it is thought that AFB1's partial negative charge, associated with the C-4 carbon atom,<sup>42</sup> has a greater attraction to NDs possessing positively charged sites. Furthermore, with the exception of the terminal furan ring, AFB1 is a planar molecule; therefore, when the negative portion of the AFB1 molecule binds to positive ND sites it may allow for a higher packing density as the molecule would sit vertically on the I6-40 substrate. Theoretical estimations of select NDs show both vertical and horizontal ori-

entations are possible. Additionally, the surface functional groups associated with I6-40 and RUDDM1-40 NDs differ, which causes a change in polarity on the surface of the NDs. Previous studies have shown that negatively charged RUDDM1 ND is rich in carboxyl groups, while positively charged I6 ND has a large presence of carbonyls and hydrocarbon residues.<sup>29,38</sup> To further examine the effects of functional groups on adsorption, I6 was modified with  $-\text{COOH}$ , resulting in a negatively charged particle, and compared to the  $-\text{COOH}$  rich RUDDM1 sample. The slight decrease in AFB1 adsorption on I6-COOH ND (Fig. 2) is consistent with the previously observed slightly lower capacity of RUDDM1 and can indicate that carboxyl groups are not favorable for AFB1 adsorption, but may interact with the partial positive charge on AFB1. Aside from electrostatic interactions between partially charged sites of AFB1 with charged ND surfaces, adsorption may be caused by pi-pi interactions between aromatic rings of AFB1 and  $\text{sp}^2$  shells on NDs, since it is known that detonation NDs always contain patches of  $\text{sp}^2$  carbon shells on their surface.<sup>31</sup> The above series of experiments, summarized in Fig. 2, concludes that while both positively and negatively charged NDs can adsorb AFB1, the aggregate size, which influences the surface area available for binding, had the most influential role in deciding the amount of AFB1 adsorbed.

Since adsorption can be affected by porosity, porous NDs of 177 nm in diameter (obtained by HPHT sintering of DND) were also included in the studies.<sup>36</sup> The sintered diamond had a SSA of  $136 \text{ m}^2/\text{g}$  (based on argon adsorption

TABLE IV. Maximum capacity ( $Q_{\text{max}}$ ,  $\mu\text{g}/\text{mg}$ ) and equilibrium constants ( $K$ ,  $\text{mg}/\mu\text{g}$ ) of OTA on NDs (0.1 wt%) based on four Langmuir transform equations.

Transforms	I6-OH		I6-140		Ch-st	
	$Q_{\text{max}}$ ( $\mu\text{g}/\text{mg}$ )	$K$ ( $\text{mg}/\mu\text{g}$ )	$Q_{\text{max}}$ ( $\mu\text{g}/\text{mg}$ )	$K$ ( $\text{mg}/\mu\text{g}$ )	$Q_{\text{max}}$ ( $\mu\text{g}/\text{mg}$ )	$K$ ( $\text{mg}/\mu\text{g}$ )
Eadie-Hofstee	24.821	17.731	20.626	7.974	15.847	1.531
Lineweaver-Burk	24.510	18.545	20.121	8.569	15.949	1.507
Reciprocal Line	26.247	14.111	22.321	5.895	16.287	1.415
Scratchard	25.355	16.447	21.060	7.439	15.958	1.506
<b>Average</b>	<b>25.233</b>	<b>16.708</b>	<b>21.032</b>	<b>7.469</b>	<b>16.010</b>	<b>1.489</b>

experiments) and mesopore sizes smaller than 5 nm.<sup>36</sup> Porous samples showed a 28% improvement in adsorption capacity over the comparable sized ND aggregate, RDDM ND (SSA of  $\sim 250$  m<sup>2</sup>/g), despite an overall lower SSA. RDDM samples, which consist of dense polycrystals, lack any porosity.

It should be emphasized, that aggregates of detonation ND have an inherent porous structure.<sup>38</sup> For example, the RUDDM1 sample (SSA 319.5 m<sup>2</sup>/g) has a pore size of 6.52 nm and volume of 0.599 cc/g. Based on the data reported in the previous paragraph, it can be concluded that the presence of pores within the ND aggregates contributes to the adsorption capacities of the NDs. Loose aggregates with large pores were also formed by mixing equal portions of negatively and positively charged NDs (I6 and RUDDM1 40 nm NDs) before proceeding as normal with the toxin experiment. Aggregation of the NDs immediately took place. However, no increase in adsorption over the individualized results was observed (Fig. 2), regardless of the ability for AfB1 to electrostatically interact with both positive and negative ND surfaces. These studies emphasize the importance of pore structures and porosity in the adsorption of AfB1.

Interestingly, when ND suspensions were prepared at *pH* 2.5, adsorption capacities were preserved. This is important for enterosorbents since much of the toxin-ND interaction occurs in the stomach. However, in alkaline environments degradation of the AfB1 molecule was observed; however, peak placement did not shift (see SMFig. 1; Ref. 39). Within 30 mins approximately 53% of AfB1 was degraded in the presence of NaOH, with no greater degradation over the next 21 hs (see SMFig. 1(a); Ref. 39). It is known that in alkaline environments, the lactone ring in AfB1 is opened, thereby changing the properties of the AfB1 molecule.<sup>30</sup> Nonetheless, due to the spectral changes of AfB1 with and without NDs, it appears that NDs are still adsorbing the toxin even in the alkaline environment (SMFig. 1(b); Ref. 39).

The adsorption capacity of NDs were also affected by the concentration of ND suspensions (0.1 versus 0.5 wt. %). To further analyze these differences, volume ratios of AfB1 to ND solutions were altered from 3:7 to 1:1 and 3:1. Both the concentration increase and ratio adjustment alter the number of ND particles in the total system, which led to differences in the uptake of AfB1 molecules (Fig. 4). By increasing the amount of NDs the percentage of bound AfB1 molecules (adsorption percentage) was larger due an increased number of adsorption sites. However, this increase also corresponded to a drop in adsorption capacity. Other published work was consistent with our results and suggests there were an insufficient number of solute molecules to cover all sites on the substrate's surface.<sup>43</sup> It is also possible that since the ND concentration had increased, the inter-particle distance had decreased. This proximity difference between charged ND particles would reduce the electrostatic attraction of an AfB1 molecule to a neighboring ND particle. These complexities in the Lang-

muir isotherm show sorbent concentrations and adsorbent to adsorbate ratios can result in different maximum capacities and equilibrium constants for the same substrate, as seen in Table III. Therefore, a substrate concentration should be chosen that will reflect respectable adsorption percentages and capacities. As a result, all future studies only focus on 0.1 wt. % ND suspensions by mixing at 3:7 volume ratio (ND:AfB1).

Three NDs, including RUDDM1-40 (0.1 and 0.5 wt. %), I6-40 (0.1 wt. %) and I6-COOH (0.1 wt. %), were chosen for the construction of the Langmuir isotherm (Fig. 3). The plateaus on the isotherms indicate that the adsorption sites have reached saturation. Maximum capacities,  $Q_{\max}$ , and equilibrium constants,  $K$ , were extracted from the isotherm through linear regression curve fitting (Table III). Four transform equations were used as each shows different error tolerances and have biases towards fitting data at low or high concentration ranges.<sup>44</sup> The transform calculations confirm that higher concentrations of NDs give rise to lower maximum capacities. By using lower concentrations of ND, the calculated maximum capacities and equilibrium constants, which give insight to binding strength, more than tripled. Comparisons of 40 nm RUDDM1 and I6 show that while I6 has a larger  $Q_{\max}$  its binding strength is slightly lower, implied by its lower equilibrium constant. The lower equilibrium constant likely correlates to I6's diverse surface groups. Though I6's  $Q_{\max}$  indicates that it has an increased number of binding sites for AfB1, because of the surface group diversity, not all of these species may equally bind the molecule. Whereas, RUDDM1's fewer, but more preferential, binding sites appear to have a greater affinity to the toxin. As earlier indicated (Fig. 2), COOH groups do not show a high preference for the AfB1 molecule, this is further suggested by the lower maximum capacity and binding calculations of COOH rich NDs, like RUDDM1 and I6-COOH, as compared to unmodified I6 (Table III).

Maximum capacity values found in this research, specifically for I6-40 and RUDDM1 40, outperform other AfB1 adsorbents such as other NDs, whose capacities range from 0.011 to 0.148  $\mu\text{g}/\text{mg}$ ,<sup>30</sup> montmorillonite (1.9  $\mu\text{g}/\text{mg}$ ),<sup>45</sup> and most yeast cell walls (though some reports indicate 11  $\mu\text{g}/\text{mg}$  adsorption is achieved, in natural *pH*<sup>44</sup>),<sup>10,46,47</sup> and show similar performance when compared to some activated charcoals (10  $\mu\text{g}/\text{mg}$ ).<sup>4,45,48</sup> Other activated charcoals and HSCAS have shown capacities as high as 120 and 86  $\mu\text{g}/\text{mg}$ , respectively.<sup>45,48</sup> However, our previous studies using dye molecules indicate ND's have a much faster kinetic rate of adsorption, since binding does not rely on diffusion.<sup>38</sup>

Finally, desorption experiments were conducted to observe the binding strength of the toxins to the NDs. Studies found that NDs did not release the toxin in DI water, NaCl or CaCl<sub>2</sub> solution. Such results indicate the AfB1 adsorption is not based on ionic interactions, but possibly, hydrogen bonding or pi-pi bonding interactions with the ND. These results suggest that ND enterosorbents will bind the toxin throughout the GI tract.

## B. Ochratoxin A

OTA binding on NDs required slightly longer incubation times than for AfB1. AfB1 adsorbed on NDs in 5 mins or less, while OTA required 15 mins, though from 5 to 15 mins adsorption increased by only 6% to 10%. Though NaCl additions were omitted, due to their influence on the OTA UV-Vis spectra (SMFig. 2(a); Ref. 39), when NDs were added to the OTA-NaCl system, further reduction in the primary peak was seen, indicating adsorption is still occurring (SMFig. 2(b); Ref. 39). The peak shifting on the UV-Vis spectrum indicates the possible formation of OTA-Na<sup>+</sup> complex or dissociation of proton due to change of ionic strength.

Differences between OTA adsorption (Fig. 5) over AfB1 adsorption on NDs are immediately observed with respect to electrostatic interactions (refer to ZP on Table I). Due to the negative nature of the OTA molecule, NDs possessing positive ZPs adsorbed greater amounts of the toxin. Interestingly, our studies indicate negatively charged NDs were still able to adsorb the toxin, despite charge repulsion, while negatively charged HSCAS clay minerals, whose binding is based on electrostatics, shows little to no adsorption of OTA.<sup>45,49</sup> Though adsorption is lower in negatively charged NDs, the presence of oxygen containing groups, specifically carboxyls on I6-COOH, OZ-ND, OZ-BI and RUDDM1,<sup>38,50</sup> exhibit the reason for binding. Previous studies using charged dye molecules showed no adsorption on NDs of like charges,<sup>34,38</sup> insinuating that electrostatic interactions dominate adsorption but are not the sole mechanism. Adsorption studies on cell walls show that functional groups, including carboxyl, hydroxyl, phosphate and amino species as well as hydrophobic interactions may be responsible for binding OTA.<sup>49</sup> NDs, which are primarily hydrophilic in nature, may also possess hydrophobic patches that aid in binding.

Unlike AfB1 studies, the degree of OTA adsorption is not based on aggregate size, but instead, surface chemistry. For example, 128 nm hydroxylated NDs perform superior to hydrogenated NDs of the same size, even though I6-H carries a stronger positive ZP (68 mV over 53 mV), as seen in Fig. 5. However, NDs stemming from the same manufacturing treatments can be altered for greater adsorption by reducing aggregate size and increasing SSA (Ch-st, I6-220 and I6-140 series). The presence of pores in the porous ND sample did not help to elevate adsorption levels.

OTA was studied in acidic and basic environments to observe the preservation of adsorption capacity. In acidic conditions OTA peak shifted from 365 to 340 nm, whereas, in basic environments the peak shifted to longer wavelengths, 385 nm. Nonetheless, in both cases, the addition of NDs shows adsorption is still occurring (SMFig. 3; Ref. 39).

Select NDs, Ch-st, I6-140 and I6-OH, were chosen for isotherm construction to compare differences of aggregate sizes and surface treatments on maximum capacities. Langmuir isotherms for these three NDs (Fig. 6) can be categorized as a L1 or L2 shape, based on Giles<sup>51</sup> classification of

isotherm shapes, which indicated that the NDs are reaching or has reached a plateau. To determine if a plateau is reached the calculated  $Q_{max}$  (Table IV) should be compared to the maximum observed quantity. The perceived maximum quantities of OTA on Ch-st, I6-140 and I6-OH are 13.403, 19.731 and 22.173  $\mu\text{g}/\text{mg}$ , respectively. This signifies that 83.7, 93.8, and 87.8% of the surface capable of holding OTA have been occupied; thus, a plateau has been reached and the shape is a L2, or completed, isotherm. I6-OH and I6-140 isotherms in this case show a steep curve at the start of the isotherm, unlike Ch-st and NDs used in AfB1 adsorption; this implies a specific type of binding and saturation of that type of site.<sup>41</sup> Equilibrium constants and capacities were highest for I6-OH NDs, making it apparent that hydroxyl groups have a strong affinity for OTA molecules. However, all other NDs indicated strong binding through their calculated equilibrium constants (Table IV). Maximum capacities obtained in this research show greater affinity for OTA over clay mineral enterosorbents, including HSCAS (0–2.2  $\mu\text{g}/\text{mg}$ ) and bentonites (1.9–9.0  $\mu\text{g}/\text{mg}$ ) and yeast cell walls (2.7  $\mu\text{g}/\text{mg}$ ), but may perform inferior to some activated charcoals (100  $\mu\text{g}/\text{mg}$ ).<sup>45</sup>

Though calculations reveal high binding strengths, in the presence of NaCl and CaCl<sub>2</sub> solutions NDs showed considerable desorption of the bound OTA molecule, 25% and 26% correspondingly. By repeated redispersion of ND pellets in NaCl or CaCl<sub>2</sub> another 6% or less of the bound OTA molecules were released. This outcome further depicts ionic adsorption mechanisms for OTA's binding on NDs.

## IV. CONCLUSIONS

Results of this study show that surface modification treatments and size fractionation can significantly influence the quantity of the adsorbed toxin. In the case of AfB1, aggregate size is the major factor for adsorption capacity. NDs with the smallest aggregate sizes (40 nm) adsorb the largest amounts of AfB1. However, pore structure and size also play a role in adsorption. Additionally, it was observed that AfB1 binding remains stable in the presence of salt solutions. In OTA studies, electrostatic interactions dominate adsorption, with specific surface functional groups, i.e., hydroxyls, enhancing OTA adsorption. Positively charged NDs have about double the adsorption capacity as compared to negatively charged NDs. However, in the presence of salt, desorption of toxin was observed due to their dependency on ionic adsorption mechanisms. In both toxin studies adsorption was preserved under wide range of pH, even after the toxin molecules underwent chemical reactions due to the harsh pH environments. Furthermore, the maximum capacity and binding calculations were shown to vary with both sorbent concentrations and toxin to ND ratios. Comparisons to other reported enterosorbents, including vendor received NDs, yeast cell walls, activated charcoal, and some clay minerals, showed surface-modified NDs to have superior or comparable adsorption.



## ACKNOWLEDGMENTS

This study was supported by the Materials World Network under the National Science Foundation (Grant No. DMR-0602906). The authors would like to thank Suzanne Hens, at the International Technology Center, for her preparation of surface terminated NDs; Tatyana Feygelson, Naval Research Laboratory, for preparation of hydrogen-terminated ND; Vladamir Padalko, Alit, for samples of sintered NDs and Yury Gogotsi, Department of Materials Science and Engineering and Nanomaterials Group at Drexel University, for BET analysis. Additionally, the authors would like to acknowledge Gary Payne, Department of Plant Pathology at North Carolina State University for his useful discussions on mycotoxins.

- <sup>1</sup>G. Devegowda, B. I. R. Aravind and M. G. Morton, Australian Poultry Science Symposium, University of Sydney, Sydney, NSW, Australia, 1996 (unpublished), Vol. 8, 103–106.
- <sup>2</sup>F. Galvano, A. Ritieni, and G. Galvano, *J. Food Prot.* **64**, 120 (2001).
- <sup>3</sup>A. J. Ramos and E. Hernández, *Anim. Feed Sci. and Technol.* **62**, 263 (1996).
- <sup>4</sup>A. J. Ramos, J. Fink-Gremmels, and E. Hernandez, *J. Food Prot.* **59**, 631 (1996).
- <sup>5</sup>W. L. Bryden, *Asia Pac. J. Clin. Nutr.* **16**, 95 (2007).
- <sup>6</sup>S. Gradelet, A. M. LeBron, R. Berges, M. Suschetet, and P. Astorg, *Carcinogenesis* **19**, 403 (1998).
- <sup>7</sup>S. Gradelet, P. Astorg, A. M. LeBron, R. Berges, and M. Suschetet, *Cancer Lett.* **114**, 223 (1997).
- <sup>8</sup>H. S. Hussein and J. M. Brasel, *Toxicology* **167**, 101 (2001).
- <sup>9</sup>R. A. Squire, *Science*. **214**, 877 (1981).
- <sup>10</sup>C. V. Rensburg, "The Ameliorating Effect of Oxihumate on Aflatoxicosis in Broilers," in *Animal and Wildlife Sciences* (University of Pretoria, Pretoria, 2005).
- <sup>11</sup>A. M. Wood, "Fungal Diseases," in *Poultry Diseases* (Elsevier, New York, 2008) p. 428.
- <sup>12</sup>M. E. Smela, S. S. Currier, E. A. Bailey, and J. M. Essigmann, *Carcinogenesis* **22**, 535 (2001).
- <sup>13</sup>F. P. Guengericha, W. W. Johnson, T. Shimada, Y. F. Ueng, H. Yamazaki, and S. Langouet, *Mutat. Res.* **402**, 121 (1998).
- <sup>14</sup>V. M. Raney, T. M. Harris, and M. P. *Chem. Res. Toxicol.* **6**, 64 (1993).
- <sup>15</sup>C. C. Harris, *Carcinogenesis* **10**, 1563 (1989).
- <sup>16</sup>J. I. Pitt, *Med. Mycol.* **38**, 41 (2000).
- <sup>17</sup>M. Denli and J. F. Perez, *Toxins* **2**, 1065 (2010).
- <sup>18</sup>*International Program of Chemical Safety, Selected Mycotoxins: Ochratoxins, tricothecenes, ergot.*, Environmental Health Criteria 105, World Health Organization, Geneva, 1990, <http://www.inchem.org/documents/ehc/ehc/ehc105.htm>.
- <sup>19</sup>A. Breitholtz-Emanuelsson, M. Olsen, A. Oskarsson, I. Palminger, and K. Hult, *J. AOAC Int.* **76**, 842 (1993).
- <sup>20</sup>M. Miraglia, M. A. DeDominicis, C. Brera, S. Conneli, E. Cava, E. Menghetti, and E. Miraslia, *Nat. Toxins*, **3**, 436 (1995).
- <sup>21</sup>P. A. Murphy, P. A. S. Hendrich, C. Landgren, and C. M. Bryant, *J. Food Sci. Technol.* **71**, 51 (2006).
- <sup>22</sup>E. O'Brien and D. R. Dietrich, *Crit. Rev. Toxicol.* **35**, 33 (2005).
- <sup>23</sup>J. M. Soriano, H. Berrada, J. Blesa, J. C. Moltó and J. Mañes, *New Issues in Food Policy, Control and Research* (Nova Science, New York, 2007).
- <sup>24</sup>H. N. Mishra and C. Das, *Crit. Rev. Food Sci. Nutri.* **43**, 245 (2003).
- <sup>25</sup>J. Varga, S. Kocsube, Z. Peteri, C. Vagvolgyi, and B. Toth, *Toxins* **2**, 1718 (2010).
- <sup>26</sup>P. M. Scott, *Food Addit. Contam.* **13**, 19 (1996).
- <sup>27</sup>M. Peraica, A. M. Domijan, Z. Jurjevic, and B. Cvjetkovic, *Arh. Hig. Rada. Toksikol.* **53**, 229 (2002).
- <sup>28</sup>T. Edrington, S. L. F. Kubena, R. B. Harvey, and G. E. Rottinghaus, *Poult. Sci.* **76**, 1205 (1997).
- <sup>29</sup>N. Gibson, O. Shenderova, T. J. M. Luo, S. Moseenkov, V. Bondar, A. Puzyr, K. Purtov, Z. Fitzgerald, and D. W. Brenner, *Diamond Relat. Mater.* **18**, 620 (2009).
- <sup>30</sup>A. P. Puzyr, K. V. Purtov, O. A. Shenderova, M. Luo, D. W. Brenner, and V. S. Bondar, *Doklady Biochem. Biophys.* **417**, 299 (2007).
- <sup>31</sup>A. M. Schrand, S. A. C. Hens and O. A. Shenderova, *CRC Crit. Rev. Solid State Mater. Sci.* **34**, 18 (2009).
- <sup>32</sup>A. M. Schrand, L. Dai, J. J. Schlager, S. M. Hussain, and E. Osawa, *Diamond Relat. Mater.* **16**, 2118 (2007).
- <sup>33</sup>A. P. Puzyr, V. S. Bondar and S. E. Al, *Siberian Med. Obozrenie (Siberian Med. Rev.)* (in Russian) **4**, 19 (2004).
- <sup>34</sup>N. M. Gibson, T. J. M. Luo, O. Shenderova, Y. J. Choi, Z. Fitzgerald, and D. W. Brenner, *Diamond Relat. Mater.* **19**, 234 (2010).
- <sup>35</sup>N. M. Gibson, T. J. M. Luo, O. Shenderova, Y. J. Choi and D. W. Brenner. MRS Fall 2009 Proceedings, Report No. 1236-SS09-05, 2010.
- <sup>36</sup>G. N. Yushin, S. Osswald, V. I. Padalko, G. P. Bogatyreva, Y. Gogotsi, *Diamond Relat. Mater.* **47**, 1721 (2005).
- <sup>37</sup>S. Hens, G. Cunningham, T. Tyler, S. Moseenkov, V. Kuznetsov, and O. Shenderova, *Diamond Relat. Mater.* **17**, 1858 (2008).
- <sup>38</sup>N. M. Gibson, T. J. M. Luo, O. Shenderova, and D. W. Brenner "Electrostatically Mediated Adsorption and Binding by Nanodiamond and Nanocarbon Particles," *J. Nanopart. Res.* (to be published).
- <sup>39</sup>See supplementary material at <http://dx.doi.org/10.1116/1.3672489> for figures pertaining to adsorption studies and mycotoxin behavior under altered environmental conditions, namely, pH adjustment and NaCl additions.
- <sup>40</sup>T. D. Phillips, E. Afriyie-Gyawu, J. Williams, H. Huebner, N. A. Ankrah, D. Ofori-Adjei, P. Jolly, N. Johnson, J. Taylor, A. Marroquin-Cardona, L. Xu, L. Tang, and J. S. Wang, *Food Addit. Contam.* **25**, 134 (2008).
- <sup>41</sup>P. G. Grant and T. D. Phillips, *J. Agric. Food Chem.* **46**, 599 (1998).
- <sup>42</sup>R. Pachter and P. S. Steyn, *Mutat. Res.* **143**, 87 (1985).
- <sup>43</sup>R. Balasubramanian, S. V. Perumal, and K. Vijayaraghava. *Ind. Eng. Chem. Res.* **48**, 2093 (2009).
- <sup>44</sup>O. Sukand, R. Sukand, A. Magirin, and T. Tenno, *Environ. Sci. Pollut. Res.* **9**, 43 (2002).
- <sup>45</sup>A. Huwig, S. Freimund, O. Kappeli, and H. Dutler, *Toxicolog. Lett.* **122**, 178 (2001).
- <sup>46</sup>K. A. Dawson, J. Evans, and M. Kudupoje, *Sci. Technol. Feed Ind.*, 169, 2001.
- <sup>47</sup>M. Moschini, A. Gallo, G. Piva, and F. Masoero, *Anim. Feed Sci. Technol.* **147**, 292 (2008).
- <sup>48</sup>W. J. Decker and D. G. Corby, *Vet. Hum. Toxicol.* **22**, 388 (1980).
- <sup>49</sup>D. Ringot, B. Lerzy, K. Chaplain, J. P. Bonhoure, E. Auclair, and Y. Lardonelle, *Biores. Technol.* **98**, 1812 (2007).
- <sup>50</sup>I. Petrov, O. Shenderova, V. Grishko, V. Grichko, T. Tyler, G. Cunningham, and G. McGuire, *Diamond. Relat. Mater.* **16**, 12 (2007).
- <sup>51</sup>C. H. Giles, D. Smith, and A. Huitson, *J. Colloid Interface Sci.* **47**, 755 (2974).